International Journal of Impact Engineering 202 (2025) 105310

Contents lists available at ScienceDirect

International Journal of Impact Engineering

journal homepage: www.elsevier.com/locate/ijimpeng

Investigation of concrete constitutive models for predicting the response, damage, and residual capacity of reinforced concrete beams subject to low velocity impact

Amirmohammad Samadzad, Matthew Whelan *, Seth Cathey, Nicole Braxtan, Shenen Chen

Department of Civil and Environmental Engineering, University of North Carolina at Charlotte, 9201 University City Blvd, Charlotte, 28223, NC, USA

ARTICLE INFO

Keywords:
Impact damage
Reinforced concrete
Concrete constitutive models
LS-DYNA
Impact loading

ABSTRACT

Low velocity impact loading from accidental collisions is a common hazard for reinforced concrete components and structures used in infrastructure applications. Both the design of resilience measures and post-event forensic assessments of such structures can be supported using finite element analysis with advanced concrete constitutive models, however comparative benchmarking of available models to multiple experiments has been limited to date. This study comprehensively evaluates the performance of five concrete constitutive models – Continuous Surface Cap Model (CSCM), Karagozian and Case Concrete (KCC), Riedel–Hiermaier–Thoma (RHT), Concrete Damage Plasticity Model (CDPM), and Winfrith concrete – for analyzing the response of reinforced concrete beams to low-velocity impacts and the subsequent response of the damaged beam to static loading. The investigation includes simulation of five series of drop weight beam experiments conducted on reinforced concrete beams encompassing a range of reinforcement ratios, shear-to-flexural resistance ratios, and impact energies. The performance of each constitutive model is assessed based on comparisons with experimentally observed displacement time histories, damage patterns, and the load–displacement responses of the damaged beams under static loading. The results provide insight into the conditions under which each constitutive model replicates the experimental measurements with strong agreement when initialized with automatic parameter generation and default parameter assignments, while also identifying significant discrepancies in the nature and extent of damage predicted when using each model. This study highlights the importance of concrete constitutive model selection for accurate impact simulation and offers practical guidance for engineers and researchers in choosing appropriate constitutive models for assessing the response of reinforced concrete structures under impact loading.

1. Introduction

Reinforced concrete is used extensively in the construction of civil infrastructure, including bridges, buildings, parking decks, tunnels, and dams, as well as protective structures, such as roadside barriers. Many of these structures are susceptible to low velocity impacts due to vehicular collision, falling objects, or other accidental events. Among other approaches, detailed analysis of the response of reinforced concrete structures to impact forces can be performed using finite element analysis to either facilitate design or inform forensic analysis. While several constitutive models providing capabilities suitable for simulating the response of concrete to low velocity impacts are available in commercial software, little comprehensive guidance has been developed to aid practitioners and researchers in selecting an appropriate constitutive model and quantifying the expected confidence in the simulation results with respect to key predictions, such as peak displacement, residual displacement, and residual capacity.

This paper focuses exclusively on the response of reinforced concrete beams subjected to impacts from hard objects at low velocities, specifically below 5 m/s. This realm of dynamic response encompasses a range of accidental and environmental impact loads, including, but not limited to, those introduced by falling objects, low speed vehicular collisions, ship collisions with offshore structures, and storm-driven debris impacts. Finite element analysis incorporating advanced concrete constitutive models has been used extensively to study the response of reinforced concrete beams to low-velocity impact [1–3]. However, few studies have contrasted the performance of different established constitutive models and, furthermore, these comparisons have been limited in scope. Saini and Shafei [4] compared simulations of drop weight impact

* Corresponding author.
E-mail address: mwhelan3@charlotte.edu (M. Whelan).

https://doi.org/10.1016/j.ijimpeng.2025.105310
Received 21 December 2024; Received in revised form 12 February 2025; Accepted 9 March 2025
Available online 20 March 2025

on a single reinforced concrete beam and on a concrete filled steel tube using the Continuous Surface Cap Model (CSCM), Elasto-Plastic Damage Cap (EPDC), Karagozian and Case Concrete (KCC), and Winfrith concrete constitutive models. Comparisons to experimentally measured time histories for impact force and displacement at the midspan of the beam were the primary means of assessing the accuracy of the models. The authors concluded that the KCC model significantly overestimates midspan displacement of reinforced concrete beams at higher impact energies, while the remaining models performed similar in predicting the measured displacement with a mild underestimation. Elshazli [5] simulated the impact response of the same reinforced concrete beam for two drop heights to compare the performance of CSCM, KCC, Winfrith, and Concrete Damage Plasticity Model (CDPM). Results similar to the prior study were obtained, although the authors cautioned that the accuracy of impact force and midspan displacement predictions were dependent on the selection of hourglass coefficient. The authors also concluded that CSCM produced the most accurate predictions of crack patterns when using effective plastic strains as an indicator for the presence and severity of cracking.

The constitutive models investigated in this study are also routinely employed for the simulation of concrete components subject to high velocity projectile impacts as well as distributed impulsive loads from blast pressures. Several recent studies have directly compared the performance of multiple concrete constitutive models when employed for simulating the response under high velocity impact and blast loading. For example, Prado et al. [6] presented experimental observations of damage to reinforced concrete beams subjected to blast and compared the observations to simulations performed with the CSCM, RHT, KCC, and Winfrith constitutive models initialized with automatic parameter generation. The authors noted differences in the sensitivity of the results obtained with each constitutive model to the mesh size, as well as in the nature and severity of damage predicted by each constitutive model. The CSCM and KCC models were noted as exhibiting deformations most similar to the experiments, although the damage predicted by the KCC models were consistently over-estimated. Similarly, Cui et al. [7] investigated the suitability of the CSCM, RHT, and KCC models, initialized with automatic parameter generation, to predict the response of a reinforced concrete column to a blast load as well as the penetration of a steel projectile into a concrete target. All three constitutive models were observed to reasonably predict the structural response under blast loading and were in agreement with respect to the location and nature of the damage. However, there were significant differences in the extent of predicted damage, which was quantified by simulating axial static loading of the blast damaged column to obtain capacity estimates. The KCC model predicted the greatest reduction in capacity, while the RHT model exhibited the mildest reduction. Given significant differences in strain rates, the nature of the loading, and the prevalent use of element erosion that is not typically required to simulate concrete response to low velocity impacts, conclusions drawn about the performance of concrete constitutive models when used in blast and high velocity impact problems should not be generalized to low velocity impact.

In addition to impact response, studies have contrasted the performance of these constitutive models when employed for nonlinear static analysis. For example, Winkelbauer [8] conducted a numerical investigation into the performance of five concrete constitutive models including CSCM, KCC, Riedel–Hiermaier–Thoma (RHT), Winfrith, and CDPM. This study involved simulations of both single elements and unconfined concrete cylinders, plates, and beams under static loading conditions, including pure compression, tension, shear, and flexure. The CSCM and KCC models exhibited the strongest agreement with experimental data. Automatically generated and default parameters for these constitutive models were found to reliably replicate the experimentally observed responses.

To address the identified gap in the existing knowledge base, this paper provides a comprehensive comparison of concrete constitutive models for the analysis of reinforced concrete beams subjected to low velocity impacts. Five concrete constitutive models available in LS-DYNA are included in the study, with a focus on assessing the performance of the models when initialized with automatic generation of the constitutive model parameters. In addition to simulating the benchmark specimen used in prior comparisons, four additional reinforced concrete beam specimens are included in the simulations to investigate the constitutive models across a range of reinforcement ratios, shear to flexural resistance ratios, and impact energies. Furthermore, beyond comparing impact force and midspan displacement time histories, the paper evaluates the prediction of crack patterns, residual displacements, and residual capacity of the beams using published experimental data to assess the accuracy of the model predictions.

2. Concrete constitutive models for impact simulation

One of the motivations of this paper is to inform the numerical simulation of reinforced concrete to impact loading by users with either a cursory understanding of concrete constitutive models or a lack of available data to calibrate parameters in the available models. Consequently, only constitutive models supported by automatic parameter generation or requiring a minimal set of mechanical properties familiar to most structural engineers were considered for the study. Additionally, the constitutive models were limited to those providing strain rate enhancement, since the application area of this paper is impact. The constitutive models investigated in this study are CSCM, KCC, RHT, CDPM, and Winfrith. In this section, each constitutive model is concisely summarized with an emphasis on the physical phenomena accounted for by each model.

It is important to emphasize that the evaluation of the constitutive models within this paper is limited to their performance when initialized with automatic parameter generation for normal strength concrete. Automatic parameter generation is commonly employed with these concrete constitutive models, since information on the concrete is often limited to compressive strength and mix design, thereby precluding even simplified calibration of parameters within the constitutive models. However, the calibration of constitutive models using triaxial and dynamic test data specific to the mix used for the concrete component under investigation can enhance the fidelity [9]. For high velocity projectile impact into concrete, the use of the KCC, CSCM, RHT, and CDPM constitutive models with automatic parameter determination has been shown to produce significant variability in the predicted penetration depth. However, calibration of equation of state and Mohr–Coulomb parameters using triaxial test data can yield consistent and strong correlation with experimental measurements [10]. Likewise, Tu and Lu [11] significantly improved unrealistic crack patterns predicted by the RHT constitutive model for a concrete slab subjected to blast loading by modifying the default parameter assignments.

2.1. Continuous surface cap model (CSCM)

The development of CSCM was initiated under the National Cooperative Highway Research Program (NCHRP) to support the analysis of roadside safety structures and was first released for LS-DYNA in 2005 [12]. This constitutive model is a cap model with a smooth intersection between the failure surface and hardening cap. This surface combines the hardening compaction surface and the failure surface in a smooth and continuous form. Using a smooth intersection simplifies the numerical analysis associated with the compressive corner region between the failure surface and cap. The cap portion predicts plastic volume change due to pore collapse, with its elliptical shape generating greater plasticity onset in isotropic compression than uniaxial strain. The model is comprised of six broad formulations: elastic update, plastic update, yield surface definition, damage, strain rate dependence and kinematic hardening. The extent of damage is determined by separate brittle and ductile damage formulations, which account for

both strain softening and modulus reduction. In this model, rate effect enhancement is applied to the plasticity surface, the damage surface, and the fracture energy. The plastic consistency criterion is governed by an associated flow rule. Dilation is exhibited by the model, which is important for prediction confinement stresses and the associated increase in concrete strength and ductility due to confinement. Furthermore, this concrete model can account for shear-enhanced compaction, which leads to hardening as a result of pore compression [13]. All parameters in the model can be automatically generated in LS-DYNA based on user-specified compressive strength and maximum aggregate size, provided that the compressive strengths of the concrete is between 28 and 58 MPa [14]. CSCM has been used extensively to predict the dynamic behavior of RC structures, including slabs [15] and beams [16] subjected to low-velocity impacts.

2.2. Karagozian-case concrete model (KCC)

The KCC constitutive concrete model was first introduced by Malvar in 1997 [17]. The aim of this model was to enhance the predictive fidelity of finite element models of reinforced concrete structures subjected to blast and impact loads. The constitutive model is based on damage-dependent, partially associative plasticity formulations. The KCC concrete model utilizes separate yield, maximum, and residual strength surfaces, all of which are sensitive to hydrostatic pressure. Shear failure for this concrete model is defined by a yield surface derived from Crawford et al. [17,18]. The combination of yield and maximum strength surfaces is used to represent hardening behavior, whereas the combination of maximum and residual strength surfaces is used to represent softening response. This constitutive model separates the deviatoric and volumetric responses, leading to a decoupling of the shear and compaction behavior. The KCC model can accurately exhibit the phenomenon of shear dilatancy, which has a significant impact on the structural response, such as ductility and strength in the presence of confinement effects. Furthermore, the concrete model incorporates strain rate enhancement, which is achieved by the use of dynamic increase factor (DIF) applied to the failure surface. In LS-DYNA, the DIF factor can be user-specified as a curve or automatically calculated internally. The internally calculated DIF factor utilizes the formulation from the Comite Euro-International du Beton (CEB) model code [19] for compression and from Malvar et al. [20] for tension . LS-DYNA enables users to efficiently generate all parameters for the KCC model automatically by simply specifying the compressive strength. The KCC constitutive model has been successfully used to simulate the response of reinforced concrete panels to airplane impacts [21] and precast concrete segmental columns with unbonded prestressing tendons subjected to vehicle collision [22], with strong agreement with experimental observations.

2.3. Riedel–Hiermaier–Thoma concrete model (RHT)

The Riedel–Hiermaier–Thoma concrete model was developed at the Ernst-Mach-Institut in 1999 [23]. The RHT model utilizes initial elastic yield, failure, and residual friction limit surfaces. These limit surfaces are influenced by pressure, strain rate effects, triaxial stresses, porous compaction, hardening, and damage evolution [24]. This model defines the failure limit surfaces for compression, tension, and shear using the pressure, effective stress, and Lode angle computed from the stress invariants [25]. LS-DYNA provides an option to automatically generate all necessary parameters for this material based on user-prescribed compressive strength. The parameters are calculated internally by interpolating between those established empirically for concrete with strengths of 35 MPa and 140 MPa, as described in [26]. The RHT constitutive model has primarily been used to simulate concrete under high velocity impacts from projectiles and fragments as well as under blast pressures [27,28]. The model has demonstrated good fidelity in predicting cratering, spalling, scabbing, and projectile penetration.

2.4. Concrete Damage Plasticity Model (CDPM)

Grassl and Jirasek [29,30] developed a triaxial damage plasticity constitutive model to simulate the failure of cohesive frictional materials, including concrete and rock. This model consists of two primary components: the damage model and the plasticity model. The damage model is developed in the context of isotropic scalar damage and relates to plastic strain evolution. It is comprised of a loading function with equivalent strain and damage evolution law. The plasticity model is based on effective stress and defined by a yield function, a non-associated flow rule, and a hardening law governing the size and shape of the yield surface that includes evolution of the hardening variable. In 2013, Grassl et al. [31] developed an extension of the original model, often referred to as CDPM2. The updated version improves the modeling of cyclic loading with tension–compression transitions and high strain rates. To achieve this, two separate damage variables for tension and compression were defined. Additionally, hardening was added to the plasticity section in the post-peak regime in order to regulate the relative contributions of damage and plasticity. Furthermore, strain rate dependence was introduced into the damage function. LS-DYNA implements CDPM2 and establishes default assignments for the advanced parameters in the model. The user must specify the elastic modulus, compressive strength, tensile strength, and parameters for the tension damage model. The keyword manual provides default values for the bilinear tension damage model. Several studies have demonstrated the suitability of CDPM for simulating reinforced concrete beams under drop weight impacts [32,3].

2.5. Winfrith concrete model

The Winfrith concrete model has been developed to accurately predict the response of reinforced concrete structures subjected to dynamic loads and has been validated through a variety of impact and blast experiments [33]. This constitutive model incorporates Ottosen yielding surfaces in the plasticity portion and defines a shear failure surface with four parameters: two relate to the meridian shape, and two relate to the octahedral shape. These shape factors are derived from fitting the shear failure to experimental data, including unconfined compression, uniaxial tensile, biaxial compression, and triaxial compression tests [34]. The relationship between hydrostatic pressure and volumetric strain in this model is represented by a straight line perpendicular to the mean stress axis. This relationship is determined by non-dimensionalized volume compaction curves derived from [35]. This model also possesses the ability to capture strain rate effects, which was improved by Broadhouse and Attwood [36], and rate enhancements are applied to the elastic modulus, shear modulus, bulk modulus, unconfined compressive strength, and tensile strength. It supports mesh regularization based on fracture energy. Shear dilation is not exhibited by the Winfrith model, which limits the ability of the model to internally account for strength and ductility increases due to confinement. Use of the Winfrith concrete model in LS-DYNA requires the user to specify the elastic modulus, Poisson's ratio, compressive strength, tensile strength, aggregate size, and either fracture energy or crack width associated with zero tensile stress, depending on whether strain rate enhancement is included. In addition to the comparative studies on reinforced concrete beams previously referenced, Winfrith concrete has been used to predict the response of slabs to drop weight impact [37] and propelled impact, with good agreement to experimentally observed maximum and residual displacements, exit velocity, failure patterns, and diameter of damaged surfaces.

2.6. Comparison of constitutive models

Concrete constitutive models vary significantly in their underlying theoretical foundations and how they capture key material behaviors

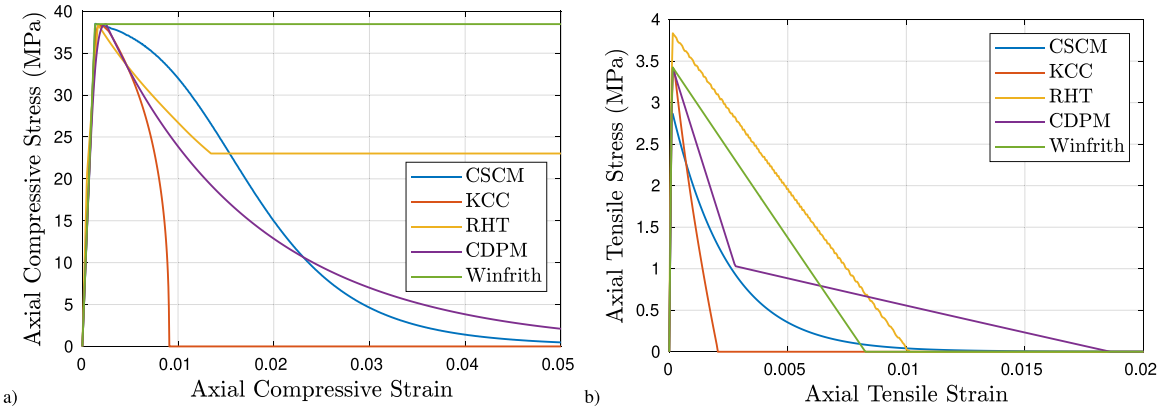

Fig. 1. Response of single hexahedral element for different constitutive models: (a) unconfined compression; (b) unconfined tension.

under loading. For instance, the CSCM concrete model considers volumetric and deviatoric behavior as coupled, while the KCC model treats these responses as decoupled. Most constitutive concrete models are a combination of various constitutive theories. Models such as CDPM, KCC, and RHT are developed based on plasticity theory and damage theory, whereas CSCM is founded on visco-plasticity theory and damage theory. Notably, the Winfrith model is also established on plasticity theory. It is important to highlight that in concrete models utilizing plasticity theory, the flow rule differs across models. For example, CSCM uses an associated flow rule, KCC allows for non-associated, partially associated, or fully associated flow, and CDPM employs a non-associated flow rule. Additionally, many strength criteria have been developed to represent the failure surface of concrete, and different models use various strength surfaces. Another significant aspect in the dynamic response of concrete is the post-peak softening behavior and shear dilation. For instance, CSCM exhibits both shear dilation and post-peak softening, while the Winfrith model does not capture shear dilation and post-peak softening in compression.

To provide insight into some of the fundamental differences between the constitutive models and to verify the correct implementation of the models by the authors, the response of a single constant stress hexahedral element with 10 mm edge size was examined with each constitutive model. In this analysis, a compressive strength of 38.4 MPa, maximum aggregate size of 10 mm, and fracture energy of 140.7 N·m/m^2 were assigned for the concrete. These values correspond to properties of the mix for the majority of the beam specimens examined later in this paper. Fig. 1a provides the response of the different constitutive models in unconfined compression. While all models exhibit similar elastic response and identical compressive strength, compression strain softening varies significantly across the models. The KCC model responds with the greatest rate of compression strain softening, while the Winfrith concrete model exhibits no compression strain softening. Fig. 1b provides the response of the constitutive models under unconfined tension. The tensile strength varies across the models, as does the fracture energy and the tensile strain at which all tensile resistance is lost. It is important to note that some of the models are sensitive to mesh size, so observations regarding the relative differences between the responses shown in Fig. 1 should not be generalized.

3. Case studies and finite element models

A set of drop weight impact and subsequent quasi-static residual capacity tests that were documented in Adhikary [38] serves as the basis for the reinforced concrete beams modeled in this paper and source for the experimental data used to assess model fidelity. These tests were conducted on reinforced concrete beams with different span-to-depth, longitudinal reinforcement, and transverse reinforcement ratios. Concise summaries of the drop weight impact and residual capacity experimental test program and results can be found in [1] and [16], respectively. In the current paper, finite element models are developed for all double reinforced specimens for which the capacities of the undamaged and impact-damaged beams were experimentally measured. These sections were denoted in the referenced literature as DR3.8-0.8-0.11, DR3.8-0.8-0.15, DR5.7-1.6-0.15, and DR5.7-1.6-0.20, where "DR" indicates doubly reinforced, 3.8 and 5.7 refer to the shear span to effective depth ratio, 0.8 and 1.6 refer to the longitudinal reinforcement ratio as a percentage, and 0.11, 0.15, and 0.20 refer to the transverse reinforcement ratio as a percentage. These beams were prepared from the same batch of concrete, for which the reported mean compressive strength was 38.4 MPa and the maximum aggregate size of the mix was 10 mm [38]. In all beams, longitudinal reinforcement was provided by 13 mm diameter deformed bars with 520 MPa yield stress and the transverse reinforcement was provided by 6 mm diameter plain bars with 310 MPa yield stress. The beam specimens with a shear span to effective depth ratio of 3.8 were subject to impact loading from a 300 kg mass dropped from heights of 60 cm, 90 cm, and 120 cm, while the beam specimens with a shear span to effective depth ratio of 5.7 were subject to impact loading from the same mass dropped from 30 cm, 45 cm, and 60 cm. All scenarios were simulated in the current paper.

In addition to the experimental data sourced from Adhikary [38], the reinforced concrete beam specimen denoted as S1616 in Fujikake et al. [39] was also modeled as a benchmark, since this specific specimen has been used extensively to investigate the modeling of reinforced concrete beams to drop weight impacts using the finite element method [4,5,40]. The compressive strength of the concrete and maximum aggregate size were reported by the authors as 42 MPa and 10 mm, respectively, so the mechanical properties of this mix are expected to be similar to those from the Adhikary [38] test program. The beam was doubly reinforced with 16 mm diameter deformed bars with 426 MPa yield strength and shear reinforcement was provided through 10 mm diameter bars with 295 MPa yield strength. The beams in this series were subject to impact loading from a 400 kg mass dropped from heights of 15 cm, 30 cm, 60 cm, and 120 cm.

The geometry and reinforcement details for all of the beam specimens sourced from the literature are presented in Fig. 2. Table 1 summarizes the longitudinal reinforcement ratio, ρ_L, calculated flexural resistance, R_M, shear resistance, R_S, and shear-to-flexural resistance ratio for the beams. In contrast to the S1616 specimen that has been used extensively as a benchmark for numerical modeling, the additional specimens have shear-to-flexural resistance ratios that approach unity. It has been experimentally observed that reinforced concrete beams that are flexure-controlled under static loads can fail in shear under impact loading and the susceptibility to shear-critical failure can be

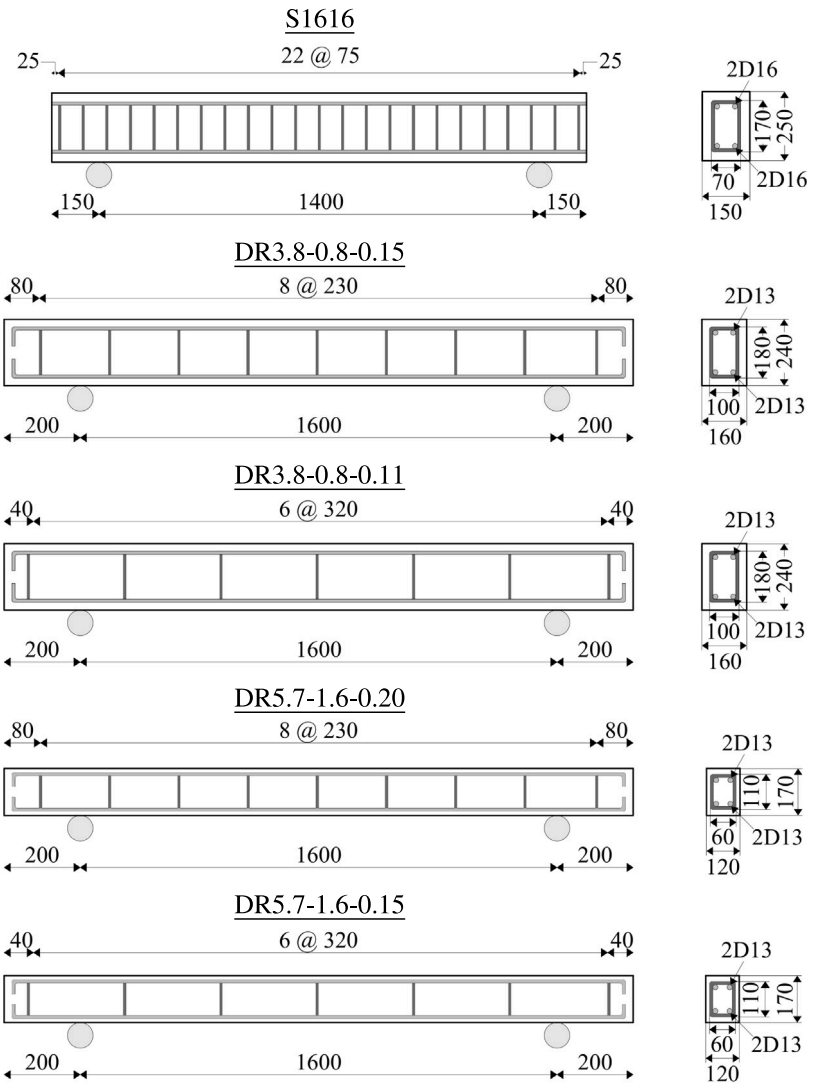

Fig. 2. Geometry and reinforcement details for beam specimens.

Table 1
Reinforcement ratios and calculated capacities of beams to concentrated loading at midspan.

Specimen	ρ_L (%)	R_M (kN)	R_S (kN)	$\frac{R_S}{R_M}$
S1616	1.26	91.1	232.0	2.55
DR3.8-0.8-0.15	0.80	67.8	102.3	1.51
DR3.8-0.8-0.11	0.80	67.8	93.3	1.38
DR5.7-1.6-0.20	1.60	42.4	56.4	1.33
DR5.7-1.6-0.15	1.60	42.4	50.5	1.19

explained by dynamic equilibrium [41]. This has also been shown to be more pronounced as the impact velocity increases and for higher velocity drop weight impacts the failure mode is typically characterized by formation of a shear plug. For the Adhikary [1] beam specimens, a steel plate was not placed at the impact location so greater impact velocities typically resulted in crushing and spalling at the impact region accompanied by flexural and flexure-shear cracking propagating from the bottom surface. However, the specimen with the lowest shear-to-flexural resistance ratio was reported to exhibit formation of a shear plug for the highest velocity impact. As a result of damage to the concrete in the compression zone, the residual static capacity of most of the specimens was reduced by the impact.

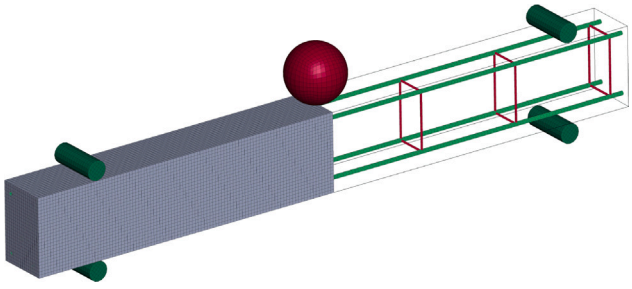

Fig. 3. Representative finite element model used in study (note: concrete elements hidden on one side of beam to show reinforcement).

3.1. Finite element modeling

Finite element analysis of the response of the reinforced concrete beams to drop weight impact and static loading was conducted using the explicit solver of LS-DYNA with all simulations performed with release 13.0.0. For all models, constant stress hexahedral solids (LS-DYNA solid element formulation 1) were used to model the beam, the supports, and the impactor. A rendering of a representative model

Table 2
Mechanical properties used to generate concrete constitutive models.

Specimen	f'_c (MPa)	d_{max} (mm)	f_t (MPa)	E_c (GPa)	G_F (N/m)	w_f (mm)
S1616	42.0	10	3.625	30.46	143.1	0.175
DR3.8-0.8-0.15	38.4	10	3.415	29.12	140.8	0.183
DR3.8-0.8-0.11	38.4	10	3.415	29.12	140.8	0.183
DR5.7-1.6-0.20	38.4	10	3.415	29.12	140.8	0.183
DR5.7-1.6-0.15	38.4	10	3.415	29.12	140.8	0.183

is provided in Fig. 3. Similar to prior studies [4], a mesh with uniform 10 mm edge size was used to develop the model of the S1616 beam specimen, which was established through a mesh convergence study that examined the effect of the mesh size on the displacement and force time histories. To maintain consistent discretization across all beam models, mesh sizes for the other beam models were established to maintain 25 rows of elements through the depth direction of the section. Consistent discretization through the depth of the cross section ensures that the flexural stress distribution is similarly approximated for beam specimens with different depths. This resulted in element sizes of 9.6 mm × 10 mm × 10 mm for the DR3.8 beams and 6.8 mm × 7.5 mm × 7.27 mm for the DR5.7 beams.

To aid in the replication of the results, a supplementary document has been provided in the Appendix of this paper that contains the material cards used for each constitutive model and each beam specimens that was modeled in this study. For all concrete constitutive models, the mass density and Poisson's ratio of the concrete were taken as 2.4×10^{-9} ton/mm^3 and 0.2, respectively. Parameters for the CSCM, KCC, and RHT constitutive models were automatically established using the unconfined compressive strength, f'_c, and maximum aggregate size, d_{max}, for the concrete, as reported by the authors of the cited experimental studies. All remaining variables in these constitutive models were taken as the default assignments, with the exception of variables related to strain rate enhancement that were invoked for the simulation of the beam response under impact loading. Automatic parameter generation is not available for the CDPM and Winfrith concrete models in LS-DYNA, but these constitutive models can be initialized using conventional mechanical properties familiar to most structural engineers, along with established default values for advanced parameters in the constitutive models. The values prescribed for each beam specimen are presented in Table 2. The tensile strength, f_t, and fracture energy, G_F, of the concrete were estimated from the unconfined compressive strength of the concrete using the CEB-FIB Model Code 2010 [19]. The elastic modulus, E_c, was similarly estimated using the empirical equation presented by ACI 318 [42]. For the CDPM constitutive model, the bi-linear damage formulation was used. The tensile threshold value, w_f, was established using the fracture energy and default assignments for the threshold values associated with the point at the transition between the two linear portions of the damage law. Element erosion was not enabled in any of the concrete constitutive models. The inclusion of erosion would introduce a strong dependency of the results on the erosion criteria and limits used, which have a wide variation throughout the literature and exhibit sensitivity to mesh size [43]. Since neither penetration of the impactor into the concrete nor fragmentation were observed in the experimental tests being simulated, the nature of the failure can be adequately predicted without erosion.

Longitudinal reinforcing bars and stirrups were modeled with Hughes–Liu beam elements with 2 × 2 Gauss quadrature integration. The mesh size for the reinforcement was set to the same size as the width of the solid elements in the longitudinal direction of the beam. Connectivity of the reinforcement to the concrete solid elements is enforced through the CONSTRAINED_BEAM_IN_SOLID constraint. This modeling approach adopts an assumption of perfect bond between the concrete and steel reinforcement. This has been accepted as a reasonable assumption for the impact response of reinforced concrete since it has been experimentally demonstrated that bond strength is significantly increased and development length significantly decreased in reinforced concrete under impact loading relative to quasi-static loading [44]. The PLASTIC_KINEMATIC material model was used to represent the constitutive behavior of all reinforcing steel with a piecewise linear elastic–plastic response with isotropic hardening. Strain rate effects were incorporated for the reinforcement using the Cowper Symonds model with parameters sourced from Cowper and Symonds [45]. The boundary conditions in the experimental test program were modeled with cylindrical parts and were included both below and above the beam to prevent uplift during rebound. A RIGID material with mechanical properties of steel for contact was used for these boundary parts and all translational degrees of freedom were restrained for the nodes in these parts. Following the modeling recommendation in Adhikary and Fujikake [1], the cylinders above the beam were positioned one millimeter above the surface to avoid the development of restraining moments at the supports. The impactor was modeled as a spherical part with a radius of 90 mm, which is consistent with the radius of the impactor reported for all of the experiments The mass density of the impactor was established to provide a total mass of 400 kg for the S1616 series and total mass of 300 kg for the DR38 and DR57 series tests. Solid elements were used for the impactor and a RIGID material assignment with motion constrained to only the vertical direction was used to replicate the drop weight test setup. The velocities associated with different drop heights were assigned using the INITIAL_VELOCITY_GENERATION card. The CONTACT_AUTOMATIC_SURFACE_TO_SURFACE algorithm was employed to model the contact between the beam specimens and the impactor as well as the contact between the beam specimens and cylindrical supports. Coulomb friction coefficients of 0.3 were assumed for both static and dynamic friction in the definition of the contact.

Prior to transient analysis of each beam specimen to the drop weight impact, dynamic relaxation was performed to introduce gravitational acceleration and develop the associated state of stress and deflection due to self-weight. Finite element analysis of the S1616 beam specimen was limited to transient analysis of the impact response, since no experimental test of the residual static capacity was performed. For the DR38 and DR57 series of specimens, transient analysis over a period of 0.12 s was performed to capture the impact response of the beam. After 0.12 s, mass proportional damping was introduced to the parts comprising the beam at approximately 95% of critical damping and the transient analysis was extended for an additional 0.1 s to attenuate any oscillations prior to the simulation of the residual static capacity load test. For the residual static capacity determination, full restart analysis was conducted to resume the simulation in the post-impact condition. The impactor and mass proportional damping were removed from the model and a rigid bar comprised of solid elements was introduced immediately above the midspan of the beam. Motion of the rigid bar was constrained to the vertical direction and prescribed a constant rate of downward displacement of 12.5 mm/s. This rate was sufficiently slow to avoid exciting the modal response of the beam. Strain rate enhancements were disabled in the concrete and steel constitutive models prior to the restart analysis. Fig. 4 provides a graphical depiction of the workflow established for the finite element analysis of the transient response of the each beam to drop weight impact followed by assessment of the residual static capacity.

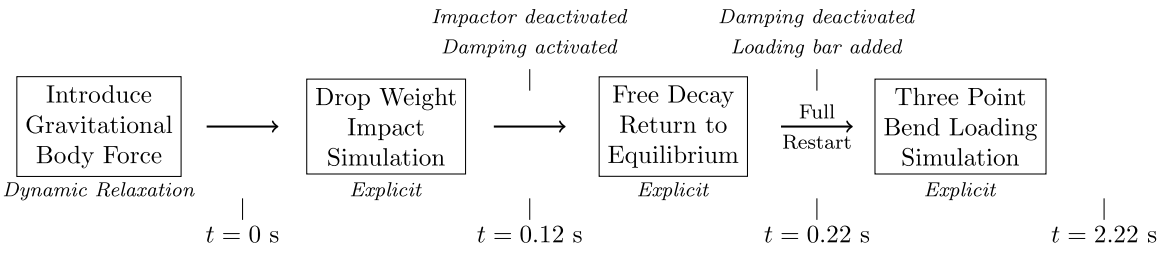

Fig. 4. Finite element analysis workflow.

3.2. Hourglass coefficients

Hourglass stabilization is necessary to suppress nonphysical hourglass modes of deformation that can occur when under-integrated solid elements are used. While the need for hourglass control and the sensitivity of transient analyses of the response of reinforced concrete under impact loading to hourglass coefficients has been discussed in prior studies [4,5], the most appropriate type of hourglass control has not been well established in the literature, with some studies utilizing stiffness forms of hourglass control [4] and others using viscous forms [1]. Prior studies comparing the performance of different constitutive models have typically determined hourglass coefficients by only comparing force and displacement time history responses to experimental data as well as evaluating the ratio of hourglass energy to internal energy. Furthermore, a common hourglass coefficient has been frequently used across all constitutive models, which may not be the most suitable choice since each constitutive model may exhibit unique sensitivity to the hourglass coefficient.

An extensive numerical simulation was conducted on the five RC beam specimens subjected to drop weight impact to arrive at selections for hourglass control type and coefficient. The Flanagan-Belytschko stiffness and viscous forms of hourglass control with exact volume integration, LS-DYNA hourglass control types 3 and 5, respectively, were each evaluated and transient analyses for all drop heights were performed for a set of eight hourglass coefficients (0.1, 0.01, 0.0075, 0.005, 0.0025, 0.001, 0.0005, and 0.0001). The ratios of hourglass energy relative to internal energy were assessed for each model to ensure that the hourglass control was not a significant source of energy dissipation in the models and to confirm conservation of total energy. Displacement time histories, force time histories, and maximum principal strain distributions were also compared to the experimental data to assess the effect of hourglass on performance of each model. Further detail on the general methodology of the hourglass sensitivity study and insight into the effect of hourglass coefficients on the simulation of reinforced concrete under low velocity impact can be found in Samadzad and Whelan [46].

To illustrate the process used to select an appropriate hourglass control type and coefficient for each concrete model, results for the S1616 beam subjected to the 120 cm height drop with the CSCM model are discussed as an example. Fig. 5 presents the maximum principal strain distributions superimposed on final deformed shape of the beam, displacement time histories, and force time histories for a subset of the hourglass coefficients evaluated. Fig. 5a depicts significant change in the maximum principal strain distributions with hourglass coefficient. Instabilities are visible in the model for the lowest coefficient, but are sufficiently suppressed when the coefficient is increased to 0.01. However, if the hourglass coefficient is further increased, the maximum principal strain distributions lose their sharpness and become smeared over the damaged region. Furthermore, the prediction of localized cracking and crushing at the top of the beam near the impact region becomes less apparent. As expected, the peak displacement at the midspan of the beam decreases with increasing hourglass coefficient, as the hourglass control effectively stiffens the structural response (Fig. 5b). Likewise, higher hourglass coefficients lead to slightly higher peak force and significantly higher oscillations in the contact force predictions (Fig. 5c). Furthermore, the ratio of hourglass energy relative to internal energy decreases as the hourglass coefficient decreases. Based on the overall responses, the coefficient of 0.01 exhibited the best correlation with the experimental data for this case. To arrive at optimal hourglass coefficients for each constitutive model, similar assessments were conducted for all drop heights across all five beam specimens. Based on the overall response, a suitable hourglass control type and coefficient were selected for each constitutive model. The most appropriate form of hourglass control was found to be the stiffness form. The hourglass coefficients were established by identifying the lowest coefficient required to suppress any visible instabilities across all of the models. By this approach, the effect of the hourglass stabilization on the result is minimized. In general, cases involving higher drop heights were more likely to exhibit instabilities and therefore controlled the selection of higher hourglass coefficients than those involving lower drop heights, but the coefficients required to suppress instabilities within the higher intensity cases were still low enough that they did not appreciably affect the results for the lower intensity cases. The optimal hourglass coefficients were determined to be 0.01 for CSCM, 0.001 for KCC, 0.0025 for RHT, 0.0075 for CDPM, and 0.001 for Winfrith. The average maximum ratio of hourglass energy to internal energy across all simulations was 0.104 for CSCM, 0.134 for KCC, 0.125 for RHT, 0.144 CDPM and 0.03 for Winfrith. It should be emphasized that these hourglass coefficients should not be generalized to other simulations, as the hourglass stabilization requirements may be dependent on the boundary conditions, load case, rate of loading, and other problem-specific parameters.

4. Assessment of constitutive models

4.1. Computational time

An important consideration in the selection of any advanced constitutive model is the computational complexity, as processor run times can increase significantly. Since each of the individual beam models analyzed in this study were nominally identical, with the exception of the assigned constitutive model and hourglass coefficient, and since all runs were performed on a dedicated high performance computing cluster, the processor time could be analyzed to provide insight into the relative computational complexity of the model implementations. The average total CPU time required for the time history analysis of the impact response of the beam was computed across all 16 combinations of beam specimen and drop height for each constitutive model. The RHT model required the least total CPU time, while KCC required only 1% more time, CSCM required 9% more time, Winfrith required 27% more time, and CDPM required 79% more time relative to RHT.

4.2. Dynamic response and residual displacement

The peak displacement and residual displacement at midspan were investigated across all beam specimens under different impact energies. Fig. 6 compares the dynamic response of each beam predicted by each constitutive model to the experimental time history measurement

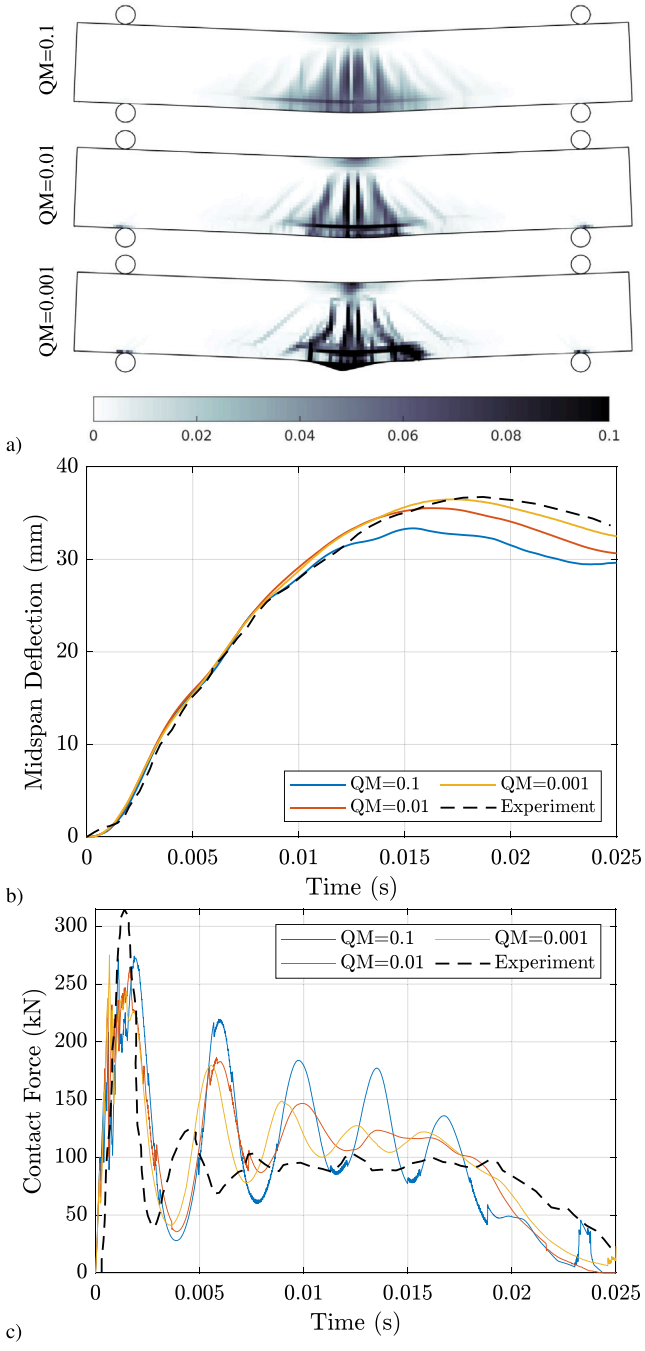

Fig. 5. Hourglass effect on DR3.8-0.8-0.11 specimen subjected to a 120 cm drop height with different hourglass coefficients using CSCM: (a) Maximum principal strain distribution; (b) Midspan displacement time history; (c) Contact force time history.

reported for each drop height. The results indicate that the peak displacement predictions are very close to the experimental data for the CSCM, RHT, and Winfrith constitutive models. On average, the peak displacement was predicted with an accuracy of approximately 3% when any of these constitutive models were used. The CSCM model consistently predicted the peak displacement well across all drop heights, as evidenced by a standard deviation in the accuracy of peak displacement prediction of approximately 5%. However, the RHT and Winfrith models exhibited a greater tendency to overpredict the peak displacement for lower drop heights and underpredict the peak displacement for higher drop heights, resulting in a larger standard deviation in accuracy of approximately 8%.

The CDPM model consistently underpredicted the peak displacement, with the extent of under prediction being sensitive to the shear-to-flexural resistance ratio. For ratios greater than 1.38, the error in average peak midspan displacement prediction was 19%, while for ratios less than 1.38, it was reduced to 6%. The KCC model was found to predict peak midspan displacement for beam specimens with shear-to-flexural resistance ratios greater than 1.50 with accuracy comparable to other models, exhibiting an average error of 6% and a standard deviation in the accuracy of 8%. However, for shear-to-flexural resistance ratios lower than 1.5, the KCC model significantly overestimated the peak midspan displacement, with errors exceeding 75% for the beam specimen with the lowest shear-to-flexural resistance ratio. It is notable that the KCC model produced accurate displacement estimates for the S1616 specimen across all drop heights, as previous studies contrasting constitutive models with this specimen have noted significant errors with KCC, particularly for larger drop heights [4,5]. The modeling approach in the current paper differs in the representation of boundary conditions and the hourglass coefficient used. Considering all specimens across all ratios for the KCC model, the average deviation is 26% with a standard deviation of 30%.

Assessment of residual midspan displacement predictions could be performed using the beam specimens from the Adhikary [16] test program since the reported displacement time histories extend sufficiently beyond the instance of peak displacement. The residual midspan displacements predicted by the Winfrith, RHT, and CDPM concrete models generally agree well with the experimental data. These models predicted the residual midspan displacement with greater accuracy for beams with lower shear-to-flexural resistance ratios, while exhibiting a tendency to underpredict the residual midspan displacement for the DR38 specimens. The CSCM constitutive model exhibited greater residual midspan displacement, typically by around 5 mm, than experimentally measured for all cases. For the DR3.8-0.8-0.15 beam specimens with shear-to-flexural resistance ratios greater than 1.50, the KCC model predicted the residual midspan displacement comparably well to the Winfrith, RHT, and CDPM models. The residual midspan displacement predicted with the KCC model typically was significantly overpredicted as the shear-to-flexural resistance ratio decreased.

4.3. Damage

Fig. 7 presents the deflected shape of the beam specimens with the maximum principal strain distributions superimposed. A consistent scale of zero to 0.1 mm/mm was used for the colormap assigned to the maximum principal strain distributions. For each subfigure, a sketch of the deflected shape with mapping of visible surface cracks and spalling was generated by drawing a layer over published photographs of each beam specimen and is provided to facilitate comparison with the damage observed in the experiments. In this figure, the results are limited to the S1616, DR3.8-0.8-0.11, and DR5.7-1.6-0.20 specimens due to space constraints and because the results obtained within the DR3.8 series and within the DR5.7 series were very similar. As previously noted, these beam specimens were subjected to direct impacts without a plate or cushion at the location of the impact. Consequently, the damage experimentally observed in the beams was characterized by flexural cracking accompanied by flexure-shear cracks and localized crushing of concrete near the impact location that progressed in severity with increased impact intensity.

The nature and severity of damage predicted by the finite element analyses varied significantly across the different constitutive models investigated, despite the generally similar displacement time history responses. Overall, the results obtained with the CSCM constitutive model exhibited damage that was most consistent with the experimental observations. The maximum principal strain distributions obtained with CSCM indicate the formation of flexure and flexure-shear cracks generally within the same portion of the span as experimentally documented as well as crushing of concrete in the compression zone localized

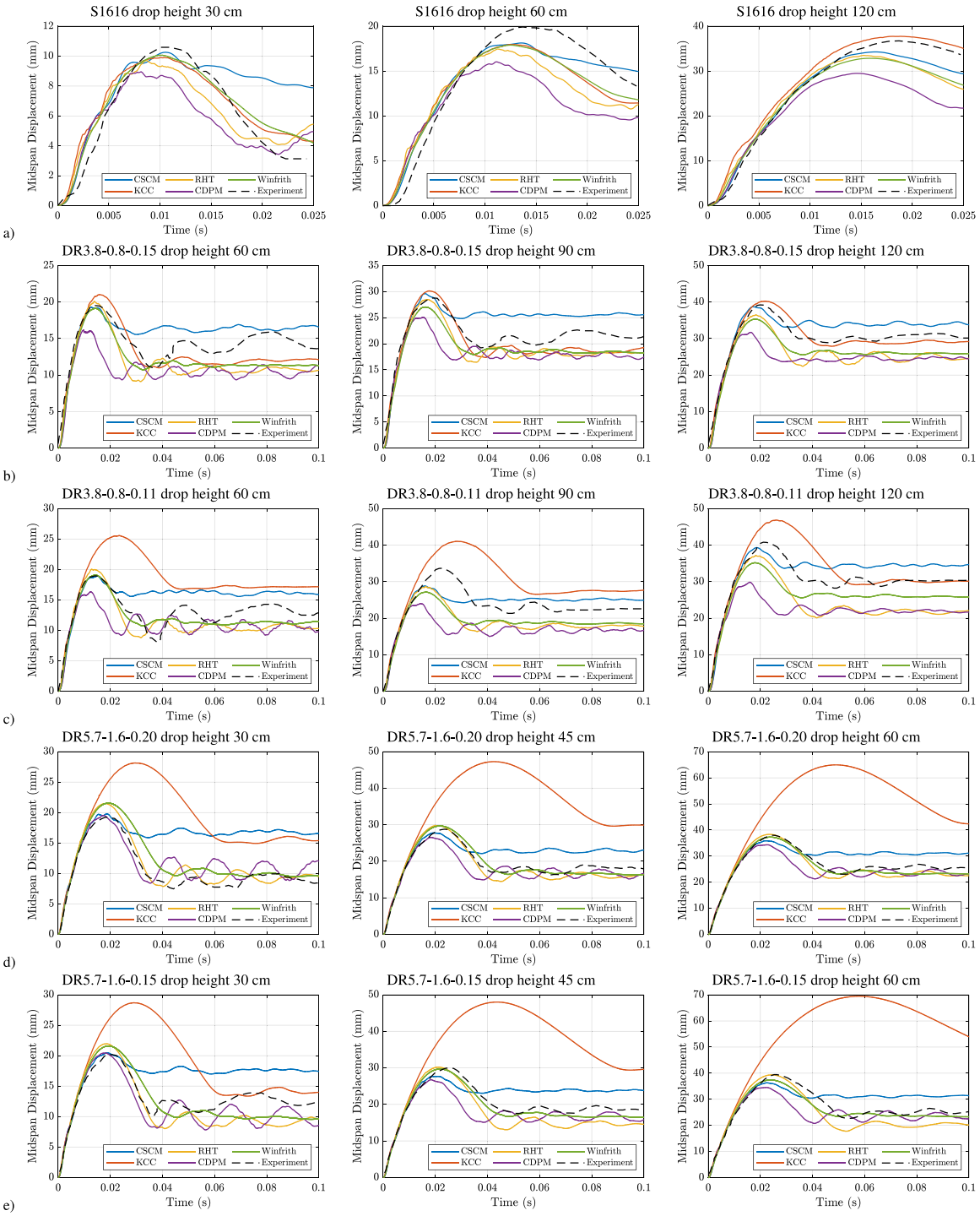

Fig. 6. Midspan displacement time histories compared to experimental measurement.

around the impact location. The observed failure mode is consistently predicted across all of the shear-to-flexure resistance ratios examined and the severity of the damage increases with impact intensity across all of the beam specimens modeled. The Winfrith concrete constitutive model produced damage predictions similar to CSCM, except that flexure-shear cracking was less pronounced and localized crushing of concrete around the location of impact was absent. The inability of the Winfrith model to predict the localized crushing of concrete is attributed to the lack of compression softening in the constitutive model. Although the RHT constitutive model consistently produced similar peak and residual displacements estimates to those obtained with the Winfrith model, the damage exhibited with the RHT model was significantly different. Across all beam specimens, the RHT model predicted only flexural cracking that was predominantly isolated to a small region at the midspan. With increased intensity of impact, the width of this region expanded and initiation of a local shear plug is reflected in the simulation results. The severity of the local shear plug development tends to increase with impact intensity, but does not appear to be affected significantly by the shear-to-flexural resistance ratio of the beam. Some degree of localized damage at the surface of impact is exhibited by the models with higher impact intensities, but the damage is less pronounced than with other constitutive models.

The KCC constitutive model similarly exhibited damage in the form of isolated flexural cracking at the midspan and a local shear plug. However, the severity of the shear plug increased significantly not only as the impact energy increased, but also as the shear-to-flexural resistance ratio of the beam decreased. Large localized deformations are particularly apparent in the simulations of the DR5.7 series specimens due to the shear failure. The absence of local shear plug failure in the experiments explains the significant discrepancy between the measured displacement time histories for this beam series and those simulated with the KCC constitutive model. Lastly, the damage exhibited by the CDPM model was characterized by flexural cracking isolated to a very narrow region at the midspan of the beam. It should be noted that prior research has shown that the use of a tetrahedral mesh is preferred over a hexahedral mesh when predicting impact damage to reinforced concrete beams with the CDPM constitutive model, as the formation of diagonal cracks may not be accurately reproduced with a hexahedral mesh [32].

The convergence study used to establish the mesh size for the models was based on displacement and force time history comparisons. To explore the effect of the mesh size on the nature and severity of damage predicted by each constitutive model, the drop weight impact analyses were performed after reducing the mesh size of each model by 50%. Consequently, in this secondary analysis, the number of rows of elements in the depth direction of the cross section was increased from 25 to 50, resulting in a element sizes of 5 mm × 5 mm × 5 mm for the S1616 beam specimen, 4.8 mm × 5 mm × 5 mm for the DR3.8 beam specimens, and 3.4 mm × 3.75 mm × 3.63 mm for the DR5.7 beam specimens. The maximum principal strain distributions are superimposed on the deflected shape for the S1616, DR3.8-0.8-0.11, and DR5.7-1.6-0.20 beam specimens in Fig. 8. In this figure, a result for the DR3.8-0.8-0.11 beam specimen with the CDPM constitutive model is not presented for 120 cm drop height because this simulation terminated prior to completion due to excessive damage. When the initial mesh size was used, the simulation performed with CDPM for this beam and drop height also exhibited extensive damage near the midspan that nearly propagated through the entire depth of section 7, so the difference in result with the finer mesh may not be significantly different. Overall, the maximum principal strain distributions across all cases are modestly sharper in resolution with the finer mesh as a result of the smaller element size, but the nature and severity of the damage inferred from the distributions is not significantly affected by the reduction in mesh size. Since the convergence study that was performed to establish the mesh size was based on displacement and force time history comparisons, this result provides evidence that convergence of the maximum principal strain distribution was also achieved with the mesh size. Further, the result, along with the low maximum ratios of hourglass energy to internal energy, suggests that the hourglass coefficients were appropriate for both mesh sizes.

4.4. Residual capacity

Predictions of the residual capacity of impact-damaged reinforced concrete structures can be used to complement visual inspections within forensic investigations and provide a means toward developing simplified tools for vulnerability assessment, such as iso-damage functions. The beam specimens examined in this study were flexure-controlled designs, which under low and moderate levels of impact loading producing only flexural and flexural shear cracking should not experience significant reductions in capacity [47]. However, when subjected to higher impact intensities, the beam specimens experienced localized crushing of concrete in the compression zone around the impact location. Consequently, the flexural stiffness, capacity, and ductility of most of the specimens were affected by the impact loading. In this section, the discussion of results is limited to the DR3.8-0.8-0.11 and DR5.7-1.6-0.20 sets of beam specimens, as those are representative of the other specimens within the DR3.8 and DR5.7 series, respectively, due to the similarity of results. Analysis of the S1616 beam specimen is excluded due to the lack of experimental data on the residual capacity of the impact-damaged beams to facilitate comparison.

The quasi-static load–displacement response of undamaged beams alongside those of impact-damaged beams, obtained experimentally and numerically using each of the constitutive models, are presented in Fig. 9. The results indicate that the flexural response for undamaged beam specimens agree well with the experimental data for all concrete models, except for the Winfrith model that overpredicted the undamaged capacity in all cases. Overall, the results highlight the challenges in predicting the residual load–displacement response of impact-damaged beams, as none of the models replicated the experimentally measured responses with high accuracy. The simulations performed using the RHT constitutive model produced the strongest correlation with the experimentally measured responses with respect to reduction in flexural capacity and ductility. However, the reduction in flexural stiffness of the impact-damaged beams was significantly overestimated. Reductions in flexural stiffness, capacity, and ductility were also predicted with the CDPM constitutive model, but the extent of these reductions was generally less than observed in the experimental tests. Simulations of the residual static response with the CSCM constitutive model did not exhibit notable changes in the flexural capacity or ductility. Similarly, the responses for the impact-damaged models using Winfrith concrete exhibited little variation and produced capacities similar to those experimentally measured for the undamaged beams. Simulations performed with the KCC constitutive model significantly over-predicted the reductions in residual stiffness and capacity. This was not unexpected due to the development of local shear plug failures and over-prediction of peak and residual midspan displacements in the simulation of the impact response of these beams using this constitutive model.

5. Conclusions

The capability of five established concrete constitutive models to predict the response and residual state of reinforced concrete beams under low velocity impacts was investigated by comprehensively comparing simulations for five different beam specimens with different shear-to-flexural resistance ratios to published experimental test data. Specifically, the use of these constitutive models with automatically generated parameters and otherwise default parameter assignments was investigated to inform practitioners with either a cursory understanding of the advanced features of the constitutive models or insufficient material test data to calibrated the parameters in these models. Analysis of the results generated the following insights that can aid researchers and practitioners in selecting a concrete constitutive model when simulating the response of reinforced concrete beams to impact loading:

- Computationally, the RHT and KCC models were found to require the least processor run time. On average, the CSCM model required an additional 9% more processor run time, while the Winfrith and CDPM models required 27% and 79% more processor run time, respectively.
- The CSCM, RHT, and Winfrith models performed the strongest in predicting the peak dynamic displacement for all beams specimens and drop heights. On average, the peak dynamic displacements were predicted within 3% of the experimentally measured values when any of these constitutive models were used. The RHT and Winfrith models did exhibit a tendency to over-predict the peak dynamic displacement at lower impact intensities and under-predict the peak dynamic displacements at higher impact intensities. The CDPM model consistently under-estimated the peak displacement by a modest amount, with greater accuracy exhibited for beams with lower shear-to-flexural resistance ratios.

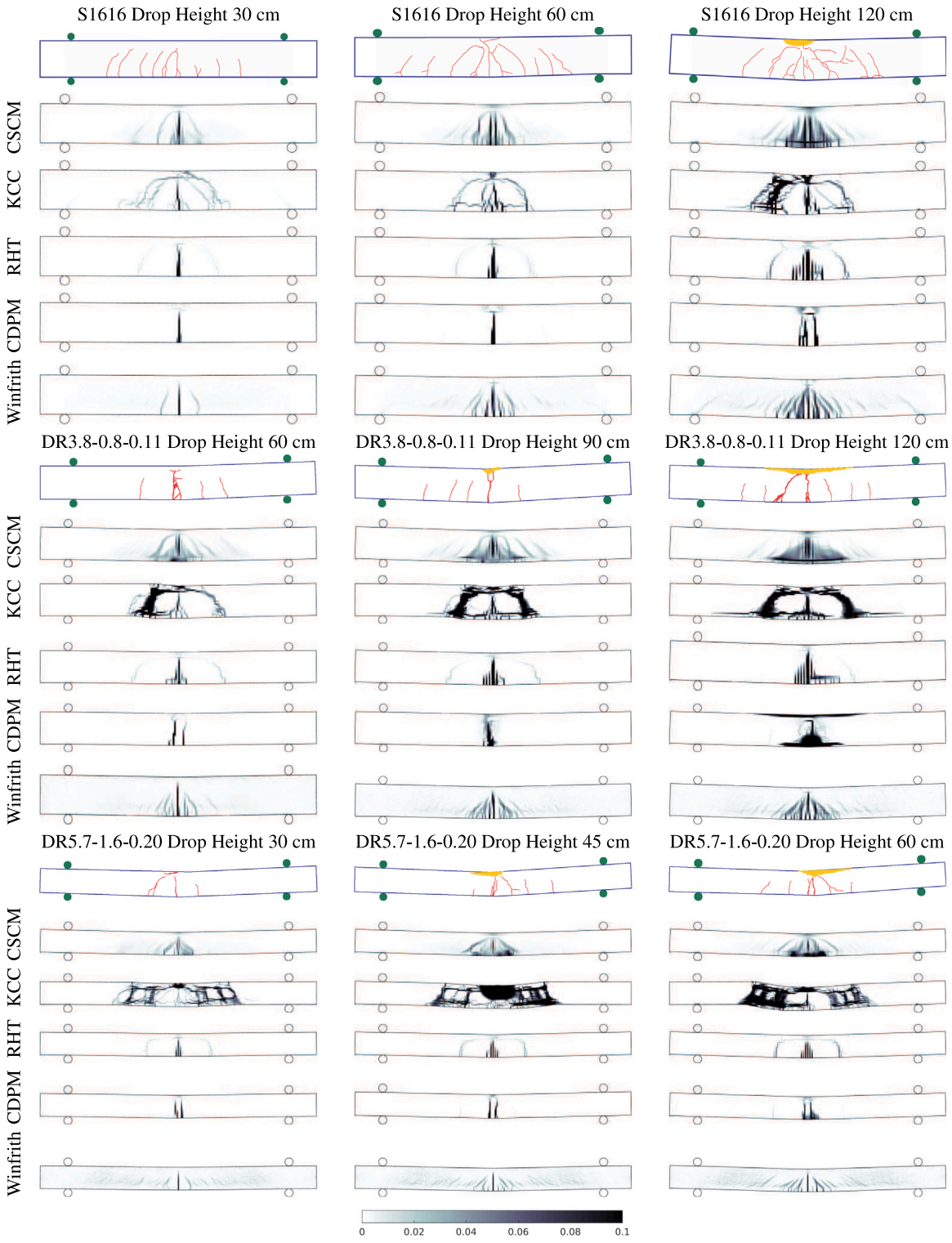

Fig. 7. Comparison between documented surface cracks from experiment and maximum principal strain distributions for each constitutive model.

The KCC model was found to be suitable for predicting the peak dynamic displacement for beams with shear-to-flexural resistance ratios greater than 1.50, but significantly over-estimated the displacement for other cases due to prediction of a local shear plug failure.

- Residual midspan displacements were predicted most accurately when using the Winfrith, RHT, and CDPM models. The simulations performed with CSCM concrete tended to moderately over-predict the residual displacement.
- Despite similarities in the predicted midspan displacement time history responses, the nature and severity of the damage predicted using each constitutive model varied significantly. The CSCM model was found to most realistically capture the flexural cracking, flexure-shear cracking, and localized crushing of concrete observed in the experiments. The Winfrith model produced similar damage predictions to CSCM, except for not being able to predict localized crushing of concrete due to the absence of compression softening. The CDPM model predicted pure flexural

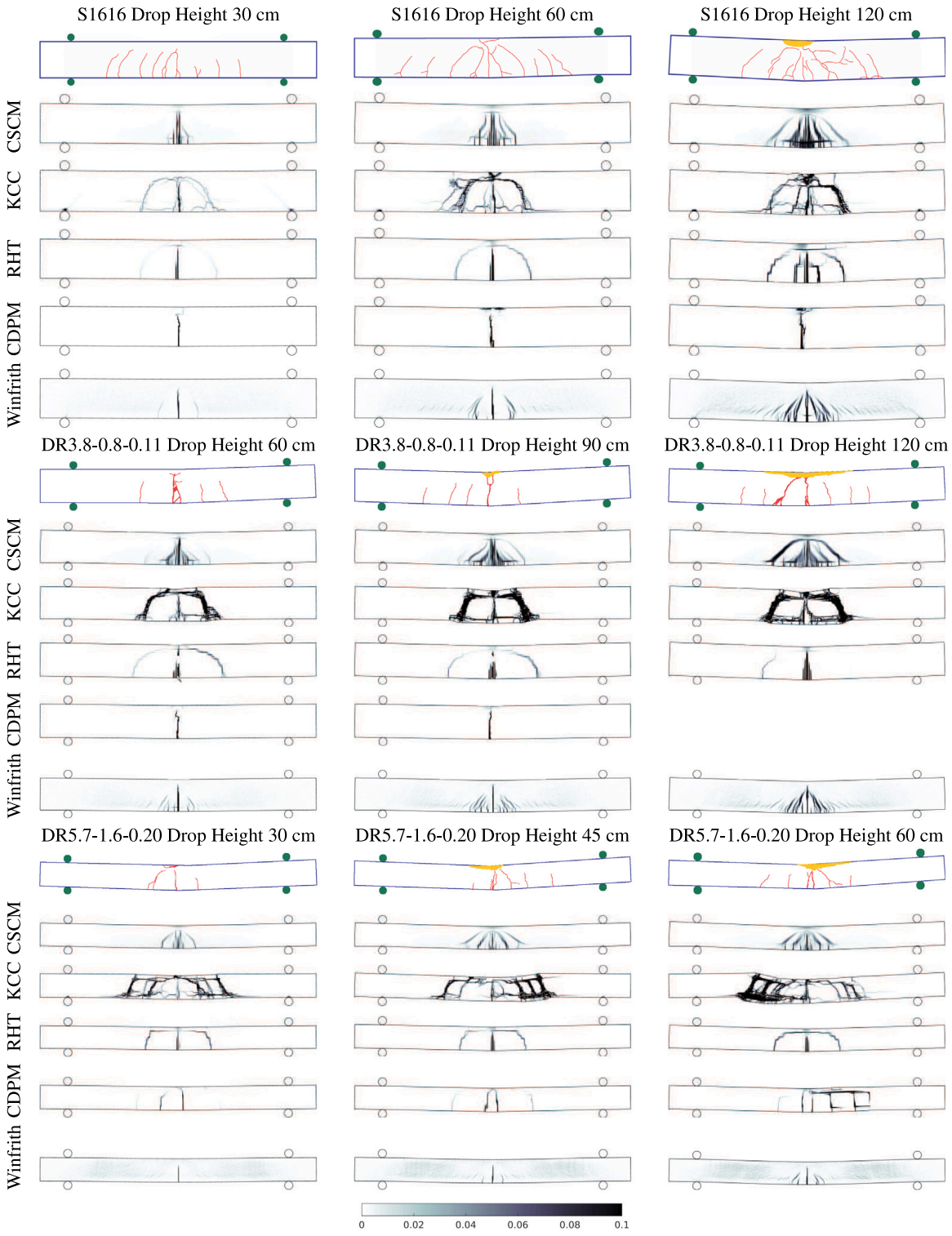

Fig. 8. Comparison between documented surface cracks from experiment and maximum principal strain distributions for each constitutive model with mesh size reduced by 50%.

failures, while the RHT and KCC models exhibited maximum principal strain distributions indicative of the initiation of a local shear plug that was not observed in the experimental test program.

- Assessment of the residual performance of the impact-damaged beams through finite element analysis with these concrete constitutive models was found to produce poor correlation with experimental measurements in most cases. However, simulations performed with the RHT model exhibited reductions in flexural capacity and ductility that most closely agreed with the measured responses.

Collectively, the RHT and CSCM models exhibited the best performance in replicating the experimental observations across all beam specimens.

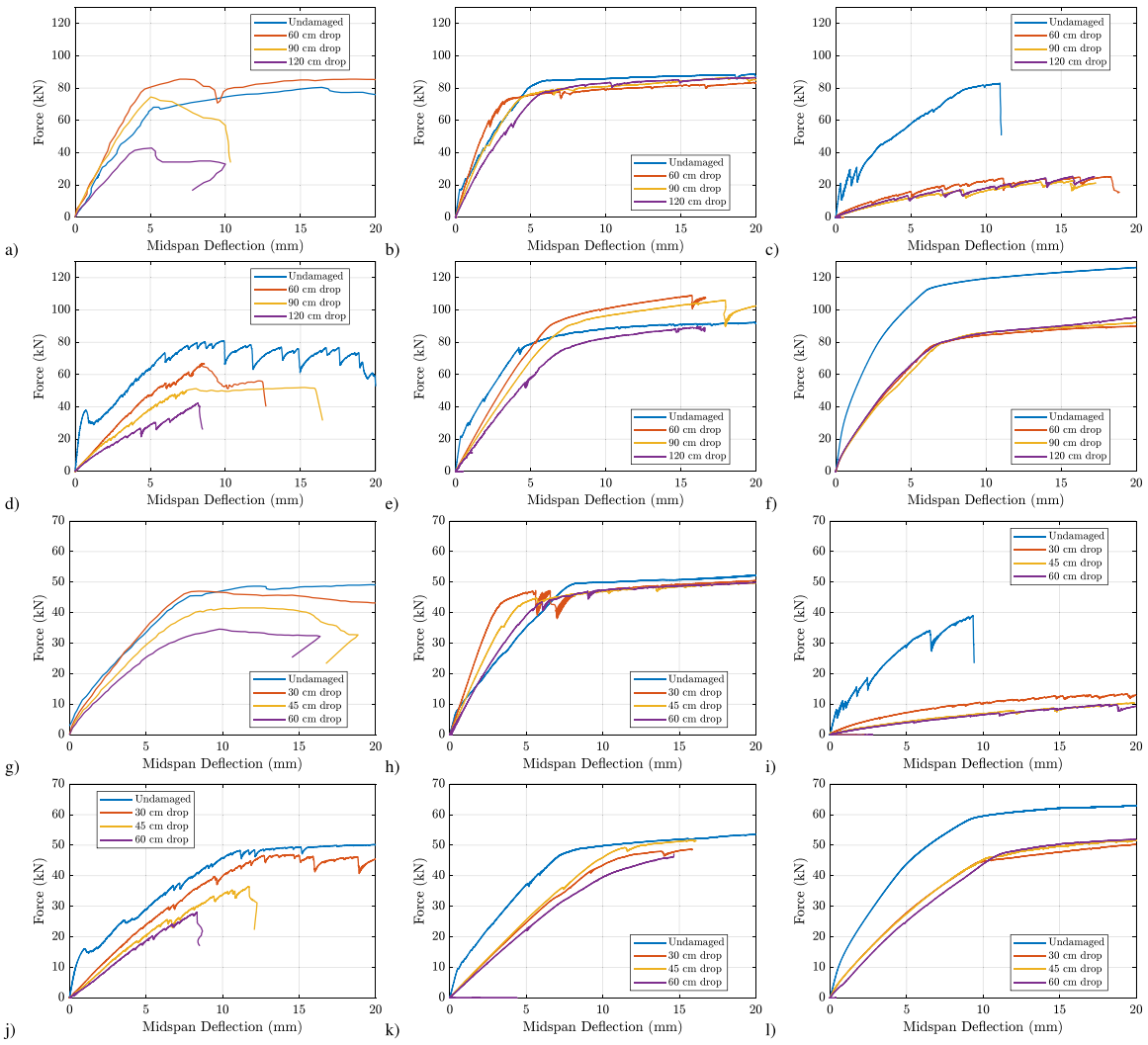

Fig. 9. Quasi-static load versus midspan displacement: (a) DR3.8-0.8-0.11 Experiment; (b) DR3.8-0.8-0.11 CSCM; (c) DR3.8-0.8-0.11 KCC; (d) DR3.8-0.8-0.11 RHT; (e) DR3.8-0.8-0.11 CDPM; (f) DR3.8-0.8-0.11 Winfrith; (g) DR5.7-1.6-0.20 Experiment; (h) DR5.7-1.6-0.20 CSCM; (i) DR5.7-1.6-0.20 KCC; (j) DR5.7-1.6-0.20 RHT; (k) DR5.7-1.6-0.20 CDPM; (l) DR5.7-1.6-0.20 Winfrith.

Simulations performed with the RHT model achieved strong agreement for peak dynamic displacement, residual displacement, and the residual static capacity and ductility. However, the nature of damage and presence and severity of cracking and spalling was not well predicted by the RHT model. Conversely, the CSCM model predicted the nature and extent of damage well, while also achieving the best agreement for peak dynamic displacement across all beam specimens. However, the residual displacement and assessment of the residual static response of impact-damaged beams with the CSCM model did not compare favorably to the experimental measurements. Additional research should be conducted to investigate how parameters in the CSCM model, such as recovery of the modulus in compression and the introduction of erosion, affect the performance, particularly to improve the ability to numerically assess the residual behavior of impact-damaged beams.

The analysis and results provided in this paper included several beam specimens encompassing a range of shear-to-flexural resistance ratios and different geometries. However, all of the beams were flexure-controlled and exhibited damage in the form of flexural cracking, flexure-shear cracking, and, in cases of higher impact intensity, localized crushing of concrete around the impact location. Extrapolating the findings to shear-controlled beams, beams exhibiting failure characterized by a local shear plug or support shear failure, or beams constructed with high performance concrete is not recommended. Future research should be directed toward evaluating the performance of concrete constitutive models for such scenarios. Lastly, the results and conclusions are specific to the use of the studied concrete constitutive models with automatic parameter generation. Potential improvements in fidelity introduced by the use of simplified techniques for calibrating constitutive model parameters using data obtained from standard concrete materials testing, such as the inverse modeling strategy recently employed by Antoniou [48] successfully used to calibrate parameters in the CSCM and RHT model for ballistic impact, should be investigated for low velocity impact problems.

CRediT authorship contribution statement

Amirmohammad Samadzad: Writing – review & editing, Writing – original draft, Visualization, Validation, Software, Investigation, Data curation. **Matthew Whelan:** Writing – review & editing, Writing – original draft, Visualization, Supervision, Methodology, Investigation, Funding acquisition, Conceptualization. **Seth Cathey:** Writing – review & editing, Validation, Investigation. **Nicole Braxtan:** Writing – review & editing, Supervision, Project administration, Methodology, Investigation, Funding acquisition. **Shenen Chen:** Writing – review & editing, Supervision, Investigation, Funding acquisition.

Declaration of competing interest

The authors declare the following financial interests/personal relationships which may be considered as potential competing interests: All authors report financial support provided by the North Carolina Department of Transportation.

Acknowledgments

The study was performed as a part of Research Project Number RP2023-06 sponsored by the North Carolina Department of Transportation, United States. The contents of this paper reflect the views of the authors and not necessarily the views of the NCDOT. The authors are responsible for the accuracy of the data presented herein. Additionally, this paper does not constitute a standard, specification, or regulation and does not necessarily reflect official policies of NCDOT. The research was accelerated by using the High Performance Computing resources developed and maintained by University Research Computing at the University of North Carolina at Charlotte.

Appendix A. Supplementary data

Supplementary material related to this article can be found online at https://doi.org/10.1016/j.ijimpeng.2025.105310.

Data availability

Data will be made available on request.

References

[1] Adhikary SD, Li B, Fujikake K. Low velocity impact response of reinforced concrete beams: Experimental and numerical investigation. Int J Prot Struct 2015;6(1):81–111. http://dx.doi.org/10.1260/2041-4196.6.1.81.
[2] Adhikary SD, Li B, Fujikake K. Dynamic behavior of reinforced concrete beams under varying rates of concentrated loading. Int J Impact Eng 2012;47:24–38. http://dx.doi.org/10.1016/j.ijimpeng.2012.02.001.
[3] Grassl P, Johansson M, Leppänen J. On the numerical modelling of bond for the failure analysis of reinforced concrete. Eng Fract Mech 2018;189:13–26. http://dx.doi.org/10.1016/j.engfracmech.2017.10.008.
[4] Saini D, Shafei B. Concrete constitutive models for low velocity impact simulations. Int J Impact Eng 2019;132:103329. http://dx.doi.org/10.1016/j.ijimpeng.2019.103329.
[5] Elshazli M, Abdulazeez M, ElGawady M, Ibrahim A. Comprehensive numerical modeling of prestressed girder bridges under low-velocity impact. Buildings 2024;14(3):1–32. http://dx.doi.org/10.3390/buildings14030640.
[6] Prado A, Alañón A, Castedo R, Santos A, López L, Chiquito M, et al. Resistance of full-scale beams against close-in explosions. Numerical modeling and field tests. Def Technol 2024;40:35–47. http://dx.doi.org/10.1016/j.dt.2024.05.002.
[7] Cui J, Hao H, Shi Y. Discussion on the suitability of concrete constitutive models for high-rate response predictions of RC structures. Int J Impact Eng 2017;106:202–16. http://dx.doi.org/10.1016/j.ijimpeng.2017.04.003.
[8] Winkelbauer B. Phase I evaluation of selected concrete material models in LS-DYNA. University of Nebraska-Lincoln; 2015.
[9] Jiang H, Zhao J. Calibration of the continuous surface cap model for concrete. Finite Elem Anal Des 2015;97:1–19. http://dx.doi.org/10.1016/j.finel.2014.12.002.
[10] Feldgun V, Yankelevsky D. Constitutive equations for reliable projectile penetration analysis into a concrete medium. Int J Prot Struct 2020;11(2):159–84. http://dx.doi.org/10.1177/2041419619860532.
[11] Tu Z, Lu Y. Evaluation of typical concrete material models used in hydrocodes for high dynamic response simulations. Int J Impact Eng 2009;36:132–46. http://dx.doi.org/10.1016/j.ijimpeng.2007.12.010.
[12] National Research Council. NCHRP report 350, recommended procedures for the safety performance evaluation of highway features. Report, Transportation Research Board; 1993.
[13] Murray YD. Users manual for LS-DYNA concrete material model 159. Final Report FHWA-HRT-05-062, 1257 Lake Plaza Drive, Colorado Springs, CO 80906: APTEK, Inc.; 2007, p. 89, URL https://rosap.ntl.bts.gov/view/dot/17482.
[14] Murray YD, Abu-Odeh A, Bligh R. Evaluation of LS-DYNA concrete material model 159. Report, Federal Highway Administration; 2007.
[15] Xiao Y, Li B, Fujikake K. Behavior of reinforced concrete slabs under low-velocity impact. ACI Struct J 2017;114:643–58. http://dx.doi.org/10.14359/51689565.
[16] Adhikary SD, Li B, Fujikake K. Residual resistance of impact-damaged reinforced concrete beams. Mag Concr Res 2015;67:364–78. http://dx.doi.org/10.1680/macr.14.00312.
[17] Malvar LJ, Crawford JE, Wesevich JW, Simons D. A plasticity concrete material model for DYNA3D. Int J Impact Eng 1997;19(9–10):847–73. http://dx.doi.org/10.1016/S0734-743X(97)00023-7.
[18] Crawford JE, Wu Y, Choi HJ, Magallanes JM, Lan S. User's manual and documentation for release III of the K&C concrete material model in LS-DYNA. Technical Report TR-11-36.6, Glendale, CA: Karagozian & Case; 2011.
[19] Comite Euro-International du Beton (CEB). CEB-FIP model code for concrete structures 2010. Lausanne, Switzerland: International Federation for Structural Concrete; 2013.
[20] Malvar LJ, Crawford JE. Dynamic increase factors for concrete. In: Proc., 28th DDESB seminar. Alexandria, VA: DDESB; 1998.
[21] Tsubota H, Koshika N, Mizuno J, Sanai M, Peterson B, Saito H, et al. Scale model tests of multiple barriers against aircraft impact: Part 1. experimental program and test results. In: Transactions of the 15th international conference on structural mechanics in reactor technology (sMiRT-15). Seoul, Korea; 1999.
[22] Do TV, Pham TM, Hao H. Numerical investigation of the behavior of precast concrete segmental columns subjected to vehicle collision. Eng Struct 2018;156:375–93. http://dx.doi.org/10.1016/j.engstruct.2017.11.033.
[23] Riedel W, Thoma K, Hiermaier S, Schmolinske E. Penetration of reinforced concrete by BETA-B-500 numerical analysis using a new macroscopic concrete model for hydrocodes. In: Proceedings of the 9th international symposium on the effects of munitions with structures, Vol. 315. Berlin-Strausberg Germany; 1999.
[24] Riedel W. 10 years RHT: A review of concrete modelling and hydrocode applications. Predict Model Dyn Processes: A Tribut Profr Klaus Thoma 2009;143–65.
[25] Borrvall T, Riedel W. The RHT concrete model in LS-DYNA. In: Proceedings of the 8th European LS-DYNA user conference. 2011.
[26] Riedel W. Beton unter dynamischen Lasten: Meso- und makromechanische Modelle und ihre Parameter (Ph.D. thesis), Universität der Bundeswehr München; 2004.
[27] Abdel-Kader M. Numerical predictions of the behaviour of plain concrete targets subjected to impact. Int J Prot Struct 2018;9:313–46. http://dx.doi.org/10.1177/2041419618759109.
[28] Leppänen J. Concrete subjected to projectile and fragment impacts: Modelling of crack softening and strain rate dependency in tension. Int J Impact Eng 2006;32:1828–41. http://dx.doi.org/10.1016/j.ijimpeng.2005.06.005.
[29] Grassl P, Jirásek M. Damage-plastic model for concrete failure. Int J Solids Struct 2006;43(22):7166–96. http://dx.doi.org/10.1016/j.ijsolstr.2006.06.032.
[30] Grassl P, Nystrom U, Rempling R, Gylltoft K. A damage-plasticity model for the dynamic failure of concrete. 2011, arXiv:1103.1288.
[31] Grassl P, Xenos D, Nyström U, Rempling R, Gylltoft K. CDPM2: A damage-plasticity approach to modelling the failure of concrete. Int J Solids Struct 2013;50(24):3805–16. http://dx.doi.org/10.1016/j.ijsolstr.2013.07.008.
[32] Leppänen J, Johansson M, Grassl P. On the dynamic response of reinforced concrete beams subjected to drop weight impact. Finite Elem Anal Des 2020;180:103438. http://dx.doi.org/10.1016/j.finel.2020.103438.
[33] Broadhouse B. The Winfrith concrete model in LS-DYNA3D. Saf Perform Dept, At Energy AuthorityTechnology, Winfrith, UK 1995.
[34] Ottosen N. A failure criterion for concrete. J Eng Mech 1977;103:527–35. http://dx.doi.org/10.1061/JMCEA3.0002248.
[35] Green SJ, Swanson SR. Static constitutive relations for concrete. Technical Report AFWL-YR-72-244, Air Force Weapons Laboratory; 1973.
[36] Broadhouse B, Attwood G. Finite element analysis of the impact response of reinforced concrete structures using DYNA3D. In: Transactions of the 12th international conference on structural mechanics in reactor technology. volume j: Structural dynamics and extreme loads analysis. 1993, p. 339–44.
[37] Sangi A, May I. High-mass, low-velocity impacts on reinforced concrete slabs. In: 7th European LS-DYNA conference. 2009.
[38] Adhikary SD. Dynamic behavior of reinforced concrete beams under varying rates of concentrated and impact loadings (Ph.D. thesis), Nanyang Technological University, Singapore; 2014.
[39] Fujikake K, Li B, Soeun S. Impact response of reinforced concrete beam and its analytical evaluation. J Struct Eng 2009;135(8):938–50. http://dx.doi.org/10.1061/(ASCE)ST.1943-541X.0000039.
[40] He Y, Fan W. Plastic-damage cap model with crack closure behavior for concrete modeling. J Eng Mech 2022;148(11):04022067. http://dx.doi.org/10.1061/(ASCE)EM.1943-7889.0002161.
[41] Saatci S, Vecchio FJ. Effects of shear mechanisms on impact behavior of reinforced concrete beams. ACI Struct J 2009;106(1):78. http://dx.doi.org/10.14359/56286.
[42] American Concrete Institute. ACI 318-19 building code requirements for structural concrete and commentary. American Concrete Institute; 2019.
[43] Luccioni B, Aráoz G, Labanda N. Defining erosion limit for concrete. Int J Prot Struct 2013;4(3):315–40. http://dx.doi.org/10.1260/2041-4196.4.3.315.
[44] Weathersby JH. Investigation of bond slip between concrete and steel reinforcement under dynamic loading conditions. Louisiana State University and Agricultural & Mechanical College; 2003.

[45] Cowper G, Symonds P. Strain-hardening and strain-rate effects in the impact loading of cantilever beams. Technical Report 28, Office of Naval Research; 1957.
[46] Samadzad A, Whelan M. Effect of hourglass control on LS-DYNA concrete constitutive models in low velocity impact simulations. In: 17th international LS-DYNA conference 2024. 2024.
[47] Dok G, Caglar N, Ilki A, Yilmaz C. Effect of impact loading on residual flexural capacity of high-strength reinforced concrete beams. Structures 2020;27:2466–80. http://dx.doi.org/10.1016/j.struc.2020.08.054.
[48] Antoniou A, Børvik T, Kristoffersen M. Evaluation of automatic versus material test-based calibrations of concrete models for ballistic impact simulations. Int J Prot Struct 2024;15(2):387–416. http://dx.doi.org/10.1177/20414196231164431.